Quantum wave-packet revivals in circular billiards

R. W. Robinett* and S. Heppelmann[†]

Department of Physics, The Pennsylvania State University, University Park, Pennsylvania 16802

(Received 21 February 2002; published 30 May 2002)

We examine the long-term time dependence of Gaussian wave packets in a circular infinite well (billiard) system and find that there are approximate revivals. For the special case of purely $m=0$ states (central wave packets with no momentum) the revival time is $T_{rev}^{(m=0)}=8\mu R^2/\hbar\pi$, where μ is the mass of the particle, and the revivals are almost exact. For all other wave packets, we find that $T_{rev}^{(m\neq 0)}=(\pi^2/2)T_{rev}^{(m=0)}\approx 5T_{rev}^{(m=0)}$ and the nature of the revivals becomes increasingly approximate as the average angular momentum or number of $m\neq 0$ states is increased. The dependence of the revival structure on the initial position, energy, and angular momentum of the wave packet and the connection to the energy spectrum is discussed in detail. The results are also compared to two other highly symmetrical two-dimensional infinite well geometries with exact revivals, namely, the square and equilateral triangle billiards. We also show explicitly how the classical periodicity for closed orbits in a circular billiard arises from the energy eigenvalue spectrum, using a WKB analysis.

I. INTRODUCTION

The connections between the quantized energy eigenvalue spectrum of a bound state and the classical motions of the corresponding classical system have become increasingly interesting and important as the ability to experimentally probe the quantum-classical interface has dramatically improved. Methods such as periodic orbit theory [1,2], for example, provide direct connections between the energy spectrum and the closed orbits of the classical system. The study of the time dependence of wave-packet solutions also depends critically on the energy spectrum, most especially as related to the existence of revivals (and super-revivals), wherein initially localized states that have a short-term, quasiclassical time evolution, can spread significantly over several orbits, only to re-form later in the form of a quantum revival in which the spreading reverses itself, the wave packet relocalizes, and the semiclassical periodicity is once again evident. Such revival phenomena have been observed in a wide variety of physical systems, especially in Rydberg atoms [3], and calculations exist for many other systems [4].

The archetype of a one-dimensional model system for quantum revivals is the infinite well (where such revivals are exact) and a number of analyses [5–10] have provided insight into both the short-term and long-term behavior of wave packets. Just as with many systems that depend on a single quantum number, one typically expands the energy eigenvalues (assuming integral values) about the central value used in the construction of a wave packet via

$$E(n)\approx E(n_0)+E'(n_0)(n-n_0)+\frac{1}{2}E''(n_0)(n-n_0)^2$$
$$+\frac{1}{6}E'''(n_0)(n-n_0)^3+\cdots, \qquad (1)$$

in terms of which the classical period, revival, and super-revival times are given, respectively, by

$$T_{cl}=\frac{2\pi\hbar}{|E'(n_0)|}, \quad T_{rev}=\frac{2\pi\hbar}{|E''(n_0)|/2}, \quad T_{super}=\frac{2\pi\hbar}{|E'''(n_0)|/6}. \qquad (2)$$

Systems with two quantum numbers [11,12], with energies labeled by $E(n_1,n_2)$, offer richer possibilities for wave-packet revivals and typically the long-term revival structure depends on three possible times, given by

$$T_{rev}^{(n_1)}=\frac{2\pi\hbar}{(1/2)\partial^2 E(n_1,n_2)/\partial n_1^2},$$

$$T_{rev}^{(n_2)}=\frac{2\pi\hbar}{(1/2)\partial^2 E(n_1,n_2)/\partial n_2^2}, \qquad (3)$$

and

$$T_{rev}^{(n_1,n_2)}=\frac{2\pi\hbar}{\partial^2 E(n_1,n_2)/\partial n_1\partial n_2}, \qquad (4)$$

and the revival structure depends on the interplay between these three times.

The two-dimensional generalization of the infinite well, or the two-dimensional infinite square well (billiard) of size $L\times L$, provides the simplest example of such a two quantum number system, and in this case the revival times are identical, namely,

$$T_{rev}^{(n_x)}=\frac{4mL^2}{\hbar\pi}=T_{rev}^{(n_y)} \qquad (5)$$

with no cross term present. For rectangular infinite wells with incommensurate sides ($L_x\times L_y$, $L_x/L_y\neq p/q$), the structure of the revival times may be more complex [11,12].

Another trivially related two-dimensional (2D) billiard system for which exact quantum revivals are guaranteed is

*Electronic address: rick@phys.psu.edu

[†]Electronic address: heppel@phys.psu.edu

an isosceles triangle infinite well with 45° angles. The solutions for that system can be obtained from the 2D square well (cut along the diagonal) by taking appropriate linear combinations of the form $[u_{(n_x)}(x)u_{(n_y)}(y) - u_{(n_x)}(y)u_{(n_y)}(x)]/\sqrt{2}$, which then satisfy the boundary conditions along the long side (hypotenuse) of the triangle, as long as $n_x \neq n_y$. The energy spectrum, therefore, consists of one set of 2D square-well energies, $E(n_x, n_y) = \hbar^2 \pi^2 (n_x^2 + n_y^2)/2mL^2$, but is restricted to $n_x < n_y$. The purely quadratic energy dependence guarantees that all wave packets will have the standard revival time given by Eq. (5).

A less obvious case of exact quantum revivals in a novel 2D billiard shape exists for the equilateral triangle. The energy spectrum for this system [13,14] (with side of length L) is given by

$$E(p,q) = \left(\frac{4}{3}\right)^2 \left(\frac{\hbar^2 \pi^2}{2mL^2}\right)(p^2 + q^2 - qp) \quad \text{with} \quad 1 \leqslant q \leqslant p/2,$$

(6)

with all states being degenerate (due to symmetries about obvious axes), except for those with $p = 2q$. Because of the exact quadratic dependence (with trivially related coefficients) on the two quantum numbers, there are exact revivals with a common revival time given by

$$T_{rev}^{(p)} = T_{rev}^{(q)} = T_{rev}^{(p,q)} = \frac{9mL^2}{4\hbar \pi}.$$

(7)

Given the fact that these two simple geometrical cases of 2D infinite well (billiard) systems exhibit exact quantum revivals, it is of interest to study to what extent, if any, the circular infinite well will exhibit revival structures. Just as square/rectangular [15] and spherical/circular [16] billiard geometries were among the first considered using periodic orbit theory, a comparison of the revival structure in these two distinct systems is appropriate. While qualitatively different from the equilateral triangle or square wells, one can perhaps suggestively describe these geometries as regular N-sided polygons with $N = 3$ and $N = 4$, respectively, so that the circular case we will consider here corresponds to $N = \infty$.

The ability to fabricate such billiard systems (or analogs thereof) and experimentally probe the energy spectrum or time dependence makes such a study of more than academic interest. For example, the energy-level structure and statistics of microwave cavities [17] provide an analog system to probe periodic orbit theory and statistical measures of chaotic behavior in arbitrarily shaped 2D billiard geometries. Measurements of conductance fluctuations in ballistic microstructures [18] have been tentatively used to identify frequency features in the power spectrum with specific closed orbits in a circular (and stadium) billiard. More recently, the realization of atom-optics billiards [19], with ultracold atoms in arbitrarily shaped 2D boundaries confined by optical dipole potentials, has allowed the study of various chaotic and integrable shapes such as the stadium, ellipse, and circle, again for short-term, semiclassical propagation. Motivated

by these studies, we will focus on the long-term revival structure of quantum wave packets in a circular billiard geometry.

Since the revival structure of any system depends on the quantum number dependence of the quantized energy eigenvalues, in Sec. II we discuss, in some detail, the dependence of the two-dimensional circular infinite well eigenvalues on the radial and angular-momentum quantum numbers, n_r and m. We then present in Sec. III, numerical results for the autocorrelation function for several classes of initially Gaussian wave packets in the circular well.

Based on both the energy eigenvalue analysis and our detailed wave packet simulations, for purely $m = 0$ wave packets (implying radially symmetric states, with no average momentum), we find almost exact revivals with $T_{rev}^{(m=0)} = 8\mu R^2/\hbar \pi$, where μ denotes the mass of the point particle in the circular billiard of radius R. For wave packets including $|m| \neq 0$ components, meaning any component with non-vanishing average momentum or one that is not initially localized at the center of the well, there are only approximate revivals, becoming increasingly so as the angular momentum is increased. The revival times in all these cases are $T_{rev}^{(m \neq 0)} = (\pi^2/2)T_{rev}^{(m=0)} \approx 5T_{rev}^{(m=0)}$ due to the seemingly accidental fact that $10/\pi^2 = 1.013$.

Finally, in Appendix A we point out a similarity between a pattern of special "accidentally" revival times in the 2D circular, square, and equilateral triangle wells, while in Appendix B, we show explicitly how the classical periodicity for closed orbits in the circular well arises directly from the quantum-mechanical energy spectrum, using a WKB analysis.

II. ENERGY SPECTRUM FOR THE CIRCULAR INFINITE WELL

The problem of a point particle (with mass denoted by μ, to avoid confusion with the angular-momentum quantum number m) confined to a circular infinite well of radius R is defined by the potential

$$V_C(r) = \begin{cases} 0 & \text{for } r < R, \\ \infty & \text{for } r \geqslant R. \end{cases}$$

(8)

The (unnormalized) solutions of the corresponding 2D Schrödinger equation are given by

$$\psi(r,\theta) = J_{|m|}(kr)e^{im\theta},$$

(9)

where the quantized angular-momentum values are given by $L_z = m\hbar$ for $m = 0, \pm 1, \pm 2, \ldots$ and the $J_{|m|}(kr)$ are the (regular) Bessel functions of order $|m|$.

The wave number k is related to the energy via $k = \sqrt{2\mu E/\hbar^2}$ and the energy eigenvalues are quantized by the application of the boundary conditions at the infinite wall at $r = R$, namely, $J_{|m|}(z = kR) = 0$. The quantized energies are then given by

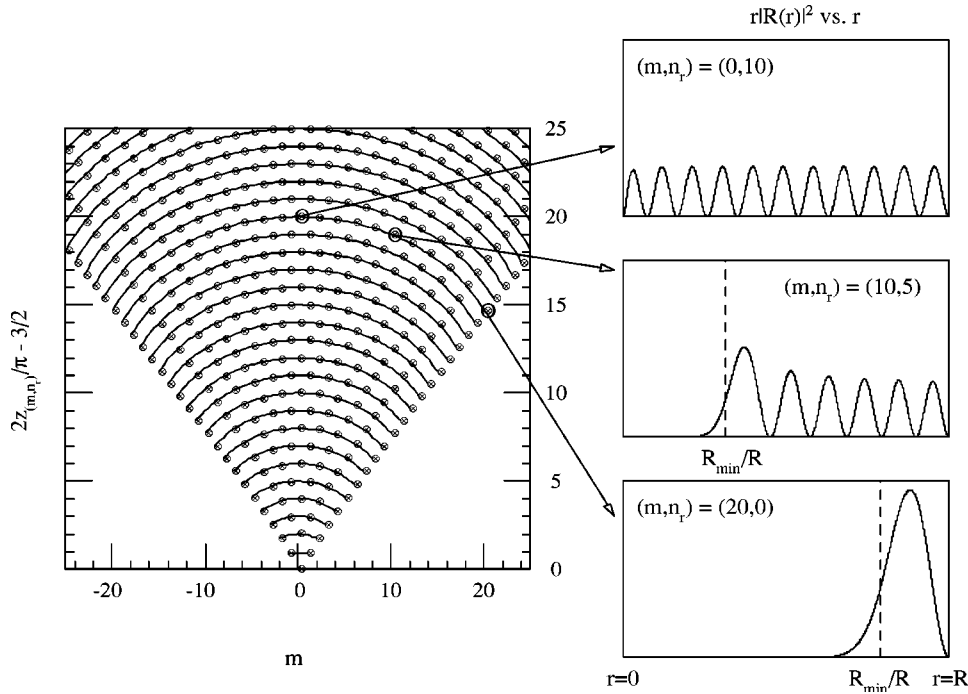$$E_{(m,n_r)} = \frac{\hbar^2 [z_{(m,n_r)}]^2}{2\mu R^2},$$

(10)

FIG. 1. Plot of the lowest-lying $z_{(m,n_r)}$ zeros of the Bessel function, determined (numerically) by $J_{|m|}(z_{(m,n_r)})=0$, vs m, scaled as $2z_{(m,n_r)}/\pi - 3/2$. Zeros corresponding to fixed values of the combination $2n_r + |m|$ are shown connected, not "fit" to data. Shown on the right are plots of the radial probability density $P(r) = r|R(r)|^2$ vs r for the three states shown with a "circle" for which a value of $2n_r + |m| = 20$ is fixed. The value of $R_{min}/R = |m|/z$ suggested by Eq. (14) is also indicated by a vertical dashed line.

where $z_{(m,n_r)}$ denotes the zeros of the Bessel function of order $|m|$ and n_r counts the number of radial nodes. The energy spectrum is doubly degenerate for $|m| \neq 0$ corresponding to the equivalence of clockwise and counterclockwise ($m>0$ and $m<0$) motion. Because the quantum number dependence of the energy eigenvalues is the determining factor in the structure of wave-packet revivals, we wish to examine the m,n_r dependence of the $E_{(m,n_r)} \propto [z_{(m,n_r)}]^2$ in detail.

As a first approximation, one can look at the large z behavior of the Bessel function solutions [20] for fixed values of $|m|$, namely,

$$J_{|m|}(z) \to \sqrt{\frac{2}{\pi z}} \cos\left(z - \frac{|m|}{2} - \frac{\pi}{4}\right) + \cdots . \qquad (11)$$

With this approximation, the zeros would be given by

$$z_{(m,n_r)} - \frac{|m|}{2} - \frac{\pi}{4} \approx (2n_r + 1)\frac{\pi}{2} \quad \text{or}$$

$$z_{(m,n_r)} \approx \left(n_r + \frac{|m|}{2} + \frac{3}{4}\right)\pi \equiv z_0(m,n_r), \qquad (12)$$

where we define the function $z_0(m,n_r)$ for future reference. If this result were exact, the quantized energies would depend on two quantum numbers in at most a quadratic manner and there would be exact wave-packet revivals, just as for the 2D square or equilateral triangle billiards.

To see to what extent this approximation is, in fact, valid for various values of m,n_r, we evaluate (numerically) a large number of the lowest-lying "exact" Bessel function zeros, $z_{(m,n_r)}$. We then plot, in Fig. 1, the combination $2z_{(m,n_r)}/\pi - 3/2$ vs m, which would yield horizontal lines

corresponding to constant, integral values of $2n_r + |m|$ if the result in Eq. (12) were exact. For three such states, we also illustrate the corresponding radial probability density and note that for increasing values of $|m|$, there are fewer radial nodes so that the appropriate values of $z = kR$ used in the boundary condition are smaller and the approximation used in Eq. (12) becomes worse.

We see that the approximation is only a good one for $|m| \approx 0$ with obvious quadratic corrections. Instead of attempting to evaluate Bessel function zeros to higher precision using more elaborate "handbook" expansions of $J_{|m|}(z)$ for large z, we note that the result of Eq. (12), and the important and necessary corrections to it, can be obtained in a straightforward and accessible way by using the WKB approximation.

If we first quantize the angular variable to find that angular momentum is given by $L_z = m\hbar$, we can note that in the radial direction the particle moves freely up to the infinite wall at $r=R$, but is subject to an effective centrifugal potential given by $V_{eff}(r) = L_z^2/2\mu r^2 = (m\hbar)^2/2\mu r^2$. The classical particle cannot penetrate this centrifugal barrier and has an associated inner radius (distance of closest approach) given by

$$V_{eff}(R_{min}) = \frac{m^2\hbar^2}{2\mu R_{min}^2} = E \quad \text{or} \quad R_{min} = \frac{|m|\hbar}{\sqrt{2\mu E}}. \qquad (13)$$

We can also write this in the useful form

$$R_{min} = \frac{|m|R}{z}, \quad \text{where} \quad E \equiv \frac{\hbar^2 z^2}{2\mu R^2}, \qquad (14)$$

more directly in terms of the desired dimensionless variable z, which is equivalent to the energy eigenvalue. In Fig. 1, we

have also indicated the value of $R_{min}/R=|m|/z$ for several of the radial probability densities, to compare to the fully quantum-mechanical results.

The WKB quantization condition on the radial variable r is then given by

$$\int_{R_{min}}^{R} k_r(r)\,dr=(n_r+C_L+C_R)\pi, \quad \text{where}$$

$$k_r(r)\equiv\sqrt{\frac{2\mu E}{\hbar^2}}\sqrt{1-\frac{R_{min}^2}{r^2}}. \quad (15)$$

The matching coefficients [21] are given by $C_L=1/4$ and $C_R=1/2$, which are appropriate for "linear" boundaries (at the inner centrifugal barrier) and "hard" or "infinite wall" boundaries (such as at $r=R$), respectively. The WKB energy quantization condition for the quantized energies, in terms of n_r explicitly and $|m|$ implicitly, via both the E and R_{min} terms, can then be written in the form

$$\sqrt{\frac{2\mu E}{\hbar^2}}\int_{R_{min}}^{R}\sqrt{1-\frac{R_{min}^2}{r^2}}\,dr=(n_r+3/4)\pi. \quad (16)$$

The integral on the left can be evaluated in the form

$$\int_{R_{min}}^{R}\sqrt{\frac{r^2-R_{min}^2}{r}}\,dr=\sqrt{R^2-R_{min}^2}-R_{min}\sec^{-1}\left(\frac{R}{R_{min}}\right)$$

$$=R[\sqrt{1-x^2}-x\sec^{-1}(1/x)], \quad (17)$$

where we define $x\equiv R_{min}/R=|m|/z$. This result can be expanded for small values of x (i.e., $R_{min}/R\ll1$ or $|m|/z\ll1$) to obtain

$$\sqrt{1-x^2}-x\sec^{-1}(1/x)=1-\frac{\pi x}{2}+\frac{x^2}{2}+\frac{x^4}{24}+\frac{x^6}{80}+\frac{5x^8}{896}$$

$$+\cdots. \quad (18)$$

The WKB quantization condition in Eq. (16) can then be written, in terms of z, in the form

$$z\left(1-\frac{\pi}{2}\frac{|m|}{z}+\frac{m^2}{2z^2}+\frac{m^4}{24z^4}+\cdots\right)=(n_r+3/4)\pi. \quad (19)$$

If we keep only the first two terms on the left-hand side, we find that

$$z\approx(n_r+|m|/2+3/4)\pi\equiv z_0(m,n_r), \quad (20)$$

which is the lowest-order result obtained directly from the limiting form of the wave function.

To improve on this result, we simply keep successively higher-order terms, solving iteratively at each level of approximation using a lower-order result for z, and we find the much improved approximation

$$z_{(m,n_r)}=z_0(m,n_r)-\frac{m^2}{2z_0(m,n_r)}-\frac{7}{24}\frac{m^4}{[z_0(m,n_r)]^3}$$

$$-\frac{83}{240}\frac{m^6}{[z_0(m,n_r)]^5}-\frac{6949m^8}{13\,440[z_0(m,n_r)]^7}+\cdots, \quad (21)$$

which we have confirmed numerically is an increasingly good approximation, especially for $n_r\gg1$. For the study of wave-packet revivals, we only require the energy eigenvalue dependence on m,n_r to second order, but higher-order terms such as those above might be useful for super-revivals and even longer-term time-dependence studies (or more detailed analytic periodic orbit theory studies of the circular well).

For the special case of $m=0$, we find no improvement using this WKB technique, but motivated by the form of the expansion in Eq. (21), we fit the first 50 lowest-lying $m=0$ zeros to a similar form and find the result

$$z_{(0,n_r)}=z_0(0,n_r)+\frac{1}{8z_0(0,n_r)}-\frac{1}{24[z_0(0,n_r)]^3}+\cdots. \quad (22)$$

We cannot unambiguously fit to any higher-order terms, as much of the nonlinear spacing information is contained in the lowest few zeros.

Using Eqs. (21) and (22), we can evaluate the energy eigenvalues to quadratic order in n_r,m in order to probe the revival structure of wave packets. For the special case of $m=0$, we find that

$$E_{(0,n_r)}=\frac{\hbar^2[z_{(0,n_r)}]^2}{2\mu R^2}=\frac{\hbar^2\pi^2}{2\mu R^2}\left[\left(n_r+\frac{3}{4}\right)^2+\frac{1}{4\pi^2}\right], \quad (23)$$

while for the more general case with $m\neq0$, we find

$$E_{(m,n_r)}=\frac{\hbar^2[z_{(m,n_r)}]^2}{2\mu R^2}=\frac{\hbar^2\pi^2}{2\mu R^2}\left[\left(n_r+\frac{|m|}{2}+\frac{3}{4}\right)^2-\frac{m^2}{\pi^2}\right]. \quad (24)$$

The fact that these energies depend on nonintegral values of the effective quantum numbers is reminiscent of the case of Rydberg wave packets in alkali-metal atoms due to quantum defects [22], and methods similar to those used there might prove useful. In what follows, however, we simply examine the time dependence of typical $m=0$ and $m\neq0$ wave packets directly.

III. GAUSSIAN WAVE PACKETS AND REVIVALS

Any wave packet in the circular billiard can be expanded in the normalized eigenstates of the form

$$\psi_{(m,n_r)}(r,\theta)=[N_{(m,n_r)}J_{|m|}(k_{(m,n_r)}r)]\left(\frac{1}{\sqrt{2\pi}}e^{im\theta}\right), \quad (25)$$

where

$$[N_{(m,n_r)}]^2 \int_0^R r \, [J_{|m|}(kr)]^2 \, dr = 1, \qquad (26)$$

with expansion coefficients given by

$$a_{(m,n_r)} = \langle \psi(r,\theta;t=0) | \psi_{(m,n_r)} \rangle, \qquad (27)$$

which satisfy

$$\sum_{m=-\infty}^{+\infty} \sum_{n_r=0}^{\infty} |a_{(m,n_r)}|^2 = 1. \qquad (28)$$

The expectation value of the energy in this potential well is given by

$$\langle \hat{E} \rangle = \sum_{m=-\infty}^{+\infty} \sum_{n_r=0}^{\infty} |a_{(m,n_r)}|^2 \left(\frac{\hbar^2 [z_{(m,n_r)}]^2}{2\mu R^2} \right), \qquad (29)$$

and the expectation values of powers of angular momentum are also easily evaluated to give

$$\langle \hat{L}_z^k \rangle = \sum_{m=-\infty}^{+\infty} \sum_{n_r=0}^{\infty} |a_{(m,n_r)}|^2 (m\hbar)^k. \qquad (30)$$

The subsequent time dependence of the wave packet is then given by

$$\psi(r,\theta;t) = \sum_{m=-\infty}^{+\infty} \sum_{n_r=0}^{\infty} a_{(m,n_r)} \psi_{(m,n_r)}(r,\theta) \, e^{-iE_{(m,n_r)}t/\hbar}, \qquad (31)$$

and the standard autocorrelation function [23] is given by

$$A(t) \equiv \langle \psi(r,\theta;t) | \psi(r,\theta,0) \rangle$$

$$= \sum_{m=-\infty}^{+\infty} \sum_{n_r=0}^{\infty} |a_{(m,n_r)}|^2 e^{-iE_{(m,n_r)}t/\hbar}. \qquad (32)$$

For definiteness, we will use a standard Gaussian wave packet of the form

$$\psi(x,y;t=0) = \psi_0(x;x_0,p_{0x},b)\psi_0(y;y_0,p_{0y},b), \qquad (33)$$

where

$$\psi_0(x;x_0,p_{0x},b) = \frac{1}{\sqrt{b(\pi)^{1/2}}} e^{ip_{0x}(x-x_0)/\hbar} e^{-(x-x_0)^2/2b^2} \qquad (34)$$

with a similar expression for $\psi_0(y;y_0,p_{0y},b)$. The initial expectation values for the x variables are given by

$$\langle x \rangle_0 = x_0, \quad \langle x^2 \rangle_0 = x_0^2 + \frac{b^2}{2}, \quad \Delta x_0 = \frac{b}{\sqrt{2}} \qquad (35)$$

and

$$\langle p_x \rangle_0 = p_{0x} \,, \quad \langle p_x^2 \rangle_0 = p_{0x}^2 + \frac{\hbar^2}{2b^2} \,, \quad \Delta p_0 = \frac{\hbar}{\sqrt{2}b}, \qquad (36)$$

with similar results for y. So long as the initial location (x_0,y_0) is well away from the edges of the potential well, such a Gaussian form can be easily and reproducibly expanded in terms of eigenstates. The expectation value of total energy is

$$\langle \hat{E} \rangle = \frac{1}{2m} \langle \hat{p}_x^2 + \hat{p}_y^2 \rangle = \frac{1}{2m} \left[(p_{0x})^2 + (p_{0y})^2 + \frac{\hbar^2}{b^2} \right]. \qquad (37)$$

In this central potential, angular momentum is conserved and we also have the specific results for this Gaussian form,

$$\langle \hat{L}_z \rangle = \langle x\hat{p}_y - y\hat{p}_x \rangle = \langle x \rangle \langle \hat{p}_y \rangle - \langle y \rangle \langle \hat{p}_x \rangle = x_0 p_{0y} - y_0 p_{0x} \qquad (38)$$

and

$$\langle \hat{L}_z^2 \rangle = (x_0 p_{0y} - y_0 p_{0x})^2 + \frac{b^2}{2}[(p_{0x})^2 + (p_{0y})^2]$$

$$+ \frac{\hbar^2}{2b^2}[(x_0)^2 + (y_0)^2], \qquad (39)$$

so that

$$(\Delta m)\hbar \equiv \Delta L_z$$

$$= \sqrt{\frac{b^2}{2}[(p_{0x})^2 + (p_{0y})^2] + \frac{\hbar^2}{2b^2}[(x_0)^2 + (y_0)^2]}. \qquad (40)$$

As a check on the numerical evaluation of the expansion coefficients, it is useful to be able to compare the general results for $\langle E \rangle$ and $\langle \hat{L}_z^{(1,2)} \rangle$ in Eqs. (29) and (30) with the specific results for the Gaussian in Eqs. (37)–(39).

We begin by focusing on the special case of zero-momentum wave packets centered at the origin, namely, with vanishing values of (p_{0x},p_{0y}) and (x_0,y_0) in which case the initial wave packet is radially symmetric and, therefore, has an expansion in pure $m=0$ angular-momentum states. [This is consistent with the result in Eq. (40), which has $\Delta L = \Delta m = 0$ for this state.]

For such states, where only the $m=0$ eigenstates contribute, we can write the energy eigenvalues from Eq. (23) in the form

$$E(n_r) = \frac{\hbar^2 \pi^2}{2\mu R^2} \left[\left(n_r + \frac{3}{4} \right)^2 + \frac{1}{4\pi^2} + O\left(\frac{1}{(n_r + 3/4)^2} \right) \right]$$

$$\approx \frac{\hbar^2 \pi^2}{32\mu R^2} \left[8n_r(2n_r + 3) + \left(9 + \frac{4}{\pi^2} \right) \right]$$

$$= \frac{\hbar^2 \pi^2}{4\mu R^2} \left[l(n_r) + \left(\frac{9}{8} + \frac{1}{2\pi^2} \right) \right], \qquad (41)$$

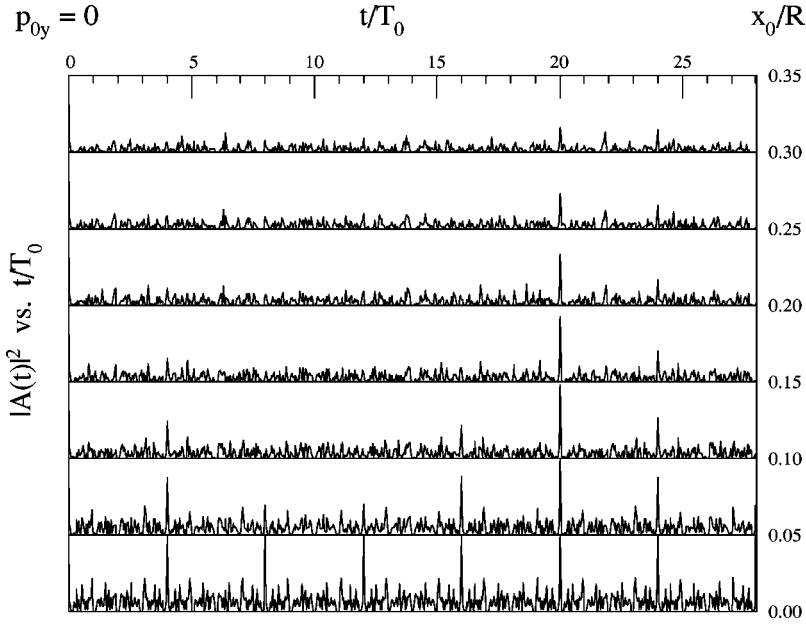$p_{0y} = 0$ t/T_0 x_0/R

FIG. 2. Plot of the autocorrelation function $|A(t)|^2$ vs t, in units of $T_0 \equiv 2\mu R^2/\hbar\pi$. The numerical values of Eq. (44) are used along with $y_0 = 0$ and $p_{0x} = p_{0y} = 0$. The results for $|A(t)|^2$ vs t, as one varies the x_0 of the initial wave packet away from the center of the circular billiard, are shown on the horizontal axes.

where $l(n_r) \equiv n_r(2n_r+3)$ is an integer (neither even nor odd, in general). The last term in the square brackets is independent of n_r and will make the same, constant, overall phase contribution to the autocorrelation function, so we focus on the $l(n_r)$ term. Since this integer has no special evenness/oddness properties, its contribution to the phase of each $|a_{(n,n_r)}|^2$ term in Eq. (32) will be identically unity at a revival time given by

$$\left(\frac{\hbar^2\pi^2}{4\mu R^2}\right)\frac{T_{rev}^{(m=0)}}{\hbar} = 2\pi \quad \text{or} \quad T_{rev}^{(m=0)} = 4\left[\frac{2\mu R^2}{\hbar\pi}\right] \equiv 4T_0.$$
(42)

Thus, at integral multiples of $4T_0$, we expect nearly perfect revivals because of the almost regularly spaced structure of the $m=0$ Bessel function zeros. At these recurrences, we can also predict the overall phase corresponding to the last term in Eq. (41), namely,

$$e^{-i\hbar^2\pi^2/4\mu R^2(4T_0)(9/8+1/2\pi^2)} = e^{-2\pi i(9/8+1/2\pi^2)}$$

$$= e^{-2\pi i}e^{-2\pi i(1/8+1/2\pi^2)} \equiv e^{-i\pi F},$$
(43)

where $F = 1/4 + 1/\pi^2 \approx 0.351$.

To investigate these predictions numerically, we have used a Gaussian of the form in Eq. (33) with the specific values

$$2m = \hbar = R = 1 \quad \text{and} \quad b = \frac{1}{10\sqrt{2}},$$

so that

$$\Delta x_0 = \Delta y_0 = 0.05. \quad (44)$$

Using the normalized eigenstates, we numerically evaluate the overlap integrals to obtain the $a_{(m,n_r)}$, using enough

states to ensure that the appropriate conditions, such as Eqs. (28)–(30), are all satisfied to better than 10^{-4} accuracy.

Using the expansion coefficients for this state, we plot the modulus squared of the autocorrelation function $|A(t)|^2$ in the bottom plots of both Figs. 2 and 3, with time "measured" in units of T_0. The almost exact revival structure at integral multiples of $4T_0$ is evident. As a further check, we can evaluate the phase of $A(t)$ at each revival and find that to an excellent approximation it is given by $-nF\pi$ as in Eq. (43). If one decreases (increases) the value of b, so that the initial wave packet is narrower (wider), the energy eigenvalues required to construct the packet are then larger (smaller) [from Eq. (37)] and are, therefore, generally more (less) evenly spaced [from Eq. (22)] and we indeed confirm this with our numerical simulations; the eventual, long-term decrease $|A(nT_0)|$ with increasing n is faster (slower) for smaller (larger) values of b.

We next move away from the special case of the zero-momentum central wave packet by considering individually the case of $x_0 \neq 0$ and $p_{0y} \neq 0$ (but not both). In each case, the average angular momentum of the state is still vanishing [from Eq. (38)], but $m \neq 0$ values of the expansion coefficients are now required. We must now use the more general case for the energies, which to second order in $m \neq 0, n_r$, are given by Eq. (24),

$$E_{(m,n_r)} = \frac{\hbar^2\pi^2}{2\mu R^2}\left[\left(n_r + \frac{|m|}{2} + \frac{3}{4}\right)^2 - \frac{m^2}{\pi^2}\right]$$

$$= \frac{\hbar^2\pi^2}{32\mu R^2}\left[(16n_r^2 + 24n_r + 16|m|n_r)\right.$$

$$\left. + 4|m|(|m|+3) - \frac{16m^2}{\pi^2}\right]$$

$$= \frac{\hbar^2\pi^2}{32\mu R^2}\left[8\tilde{l}(n_r) + 8\bar{l}(|m|) - \frac{16m^2}{\pi^2} + 9\right], \quad (45)$$

where

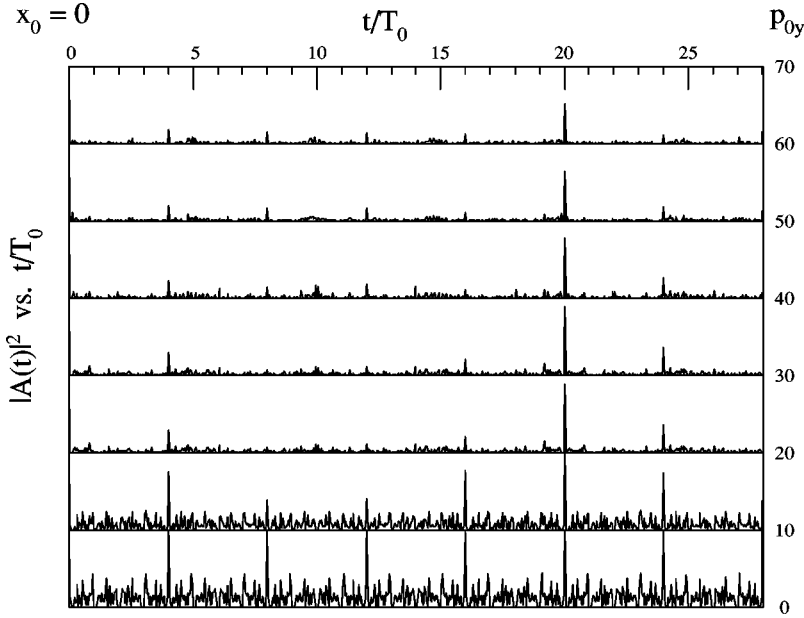$x_0 = 0$ t/T_0 p_{0y}

FIG. 3. Same as Fig. 2, but with $x_0 = y_0 = 0$ and $p_{0x} = 0$, as one increases p_{0y}.

$$\tilde{l}(n_r) \equiv n_r(2n_r + 3 + 2|m|) \quad \text{and} \quad \bar{l}(|m|) \equiv |m|(|m| + 3)/2 \tag{46}$$

are both integers, again, with no special even or oddness properties. We can then write these energies in the form

$$E_{(m,n_r)} = \frac{2\pi\hbar}{4T_0}\left[\tilde{l}(n_r) + \bar{l}(|m|) - \frac{2m^2}{\pi^2} + \frac{9}{8}\right]. \tag{47}$$

At integral multiples of the $m = 0$ revival time, $t_N = N(4T_0)$, the first two terms give $e^{-N(2\pi i)} = 1$ phases to each (m, n_r) term in the autocorrelation function, while the last term gives an overall, (m, n_r)-independent phase, just as in the $m = 0$ case. The other term, however, gives a contribution

$$e^{-(2\pi i)(m^2 N)(2/\pi^2)}, \tag{48}$$

which depends on m explicitly and which, therefore, eliminates the revivals, increasingly so, as the wave packet is dominated by $m \neq 0$ terms. However, because of a seeming numerical accident, at integral multiples of $5T_{rev}^{(m=0)} = 20T_0$, we recover approximate revivals due to the fact that $5 \times (2/\pi^2) = 1.013$. We thus find approximate revivals for the more general $m \neq 0$ case given by $T_{rev}^{(m \neq 0)} = (\pi^2/2)T_{rev}^{(m=0)} \approx 5T_{rev}^{[m=(0)]}$.

This effect is illustrated in greater detail in Figs. 2 and 3, where we plot $|A(t)|^2$ vs t as we move away from the central zero-momentum wave packet by first moving away from the origin ($x_0 \neq 0$ in Fig. 2) or from wave packets having nonzero momentum values ($p_{0y} \neq 0$ in Fig. 3). In each case, as we increase the parameter (x_0 or p_{0y}), we necessarily include more and more $|m| \neq 0$ eigenstates. For even a small mix of such states, the $T_{rev}^{(m=0)}$ revival periods at most integral multiples of $4T_0$ disappear, while evidence for the more general $T_{rev}^{(m \neq 0)} = 20T_0$ revivals remains.

For the particular numerical values used in Eq. (44), the spread in angular momentum required from Eq. (40) is given by

$$\Delta L = \sqrt{\left(\frac{p_{0y}}{20}\right)^2 + (10x_0)^2} = \Delta m \tag{49}$$

(since $\hbar = 1$), so that the $x \neq 0$ and $p_{0y} \neq 0$ values used in Figs. 2 and 3 actually correspond to the same set of ΔL for each horizontal case shown.

We note that this "lifting" of a seemingly "accidental" degeneracy in the pattern of revival times is somewhat similar to the special case of a zero-momentum Gaussian wave packet in a 2D square or triangular billiard, initially placed at the center, cases that we briefly discuss in Appendix A.

This pattern of revival times depending on two distinct quantum numbers is also somewhat reminiscent of that encountered in a rectangular billiard with differing sides of length L_x, L_y, where if the sides are incommensurate one would expect a less elaborate revival structure. Since the revival times typically scale as $T_{rev} \propto L^2$, the appearance of a π^2 scale factor that can give rise to very close to an integer ratio $10/\pi^2 \approx 1$ (to within 1.3%) is appropriate; in this case, the relevant length scales for the radial quantum number and azimuthal quantum numbers are most likely multiples of R and $2\pi R$, respectively, so that relative factors of π^2 in the revival times can appear naturally.

The presence of the $\Delta m \neq 0$ revivals becomes increasingly less obvious as the average angular momentum is increased away from zero (with both x_0 and p_{0y} now nonvanishing), since the required energy eigenvalues are in a region of large $|m|/z$, where the lowest-order approximation [from Eq. (20)] of evenly spaced z values becomes worse. We also note that even with $\langle \hat{L} \rangle = 0$, as we increase p_{0y}, the spread in m values required also increases [as in Eq. (40)], so that the overall number of states required to reproduce the initial Gaussian, and which have to "beat" against each other ap-

propriately, increases as well, making revivals more difficult to produce. The increasingly large number of states required to construct the Gaussian wave packets for larger values of $\langle \hat{L} \rangle$ can also be seen during the collapsed phase, when the "average value" of $|A(t)|^2$, namely, $\Sigma_{m,n_r}|a_{(m,n_r)}|^4$, becomes increasingly small as the fixed probability (constrained via $\Sigma_{m,n_r}|a_{(m,n_r)}|^2=1$) is spread over more and more states.

While we have focused on the long-term, revival structure of the autocorrelation function, the appearance of more short-time features in $|A(t)|$, corresponding to short-term, semiclassical closed orbits is also apparent. Such trajectories are characterized [16] by periodic orbits with path lengths and minimum radii (distances of closest approach) given by

$$L(p,q)=2pR\sin\left(\frac{\pi q}{p}\right) \quad \text{and} \quad R_{min}=R\cos\left(\frac{\pi q}{p}\right),$$

(50)

with integral values of (p,q) (with $p>2q$) describing the number of "hits" on the wall and the number of "revolutions" for one complete orbit, respectively. If, for example, we place Gaussian wave packets with $p_{0x}=0$ and $p_{0y}>0$ at locations given by $(x_0,y_0)=(R_{min}(p,q),0)$, we find obvious peaks in the autocorrelation function at times given by $T_{cl}(p,q)\equiv L(p,q)/(p_{0y}/m)$ corresponding to classical closed orbits. (This structure is evident, of course, only when the expected classical periods are less than the wave-packet spreading time Δt; this can be estimated using the result for a free Gaussian as $\Delta t=2m\Delta x_0^2/\hbar$.) We discuss in Appendix B exactly how the classical closed orbit periodicity is reproduced from the quantum-mechanical energy spectrum, using the WKB approximation of Eq. (16).

Variations of the problem of a circular infinite well can also be examined for their possible revival structure. The "half-circular" well, with an infinite wall added along a diameter, is exactly soluble with linear combinations of $e^{im\theta}$ and $e^{-im\theta}$ solutions being able to satisfy the new boundary condition for $m\neq0$, while the $m=0$ solutions are not allowed. The energy spectrum then consists of one copy of the $E_{(m\neq0,n_r)}$ values for the circular well, with a resulting revival behavior consistent with $T_{rev}^{(m\neq0)}$, since no $m=0$ states are allowed.

Another variant would be an annular circular billiard, with an inner infinite wall at $r=R_{inner}<R$. The energy eigenstates can also be derived using Bessel function solutions [now including the "irregular" or divergent $Y_{|m|}(kr)$ terms since the particle is kept explicitly away from the origin by the inner wall] with the energy eigenvalues resulting from the condition

$$J_{|m|}(kR)Y_{|m|}(kR_{inner})-J_{|m|}(kR_{inner})Y_{|m|}(kR)=0.$$

(51)

WKB-type expansions for the quantized energies are also useful in this case. The qualitatively different features present in this geometry include not only classical orbits (bouncing off the inner wall) but also diffraction features, as seen in periodic orbit theory analyses [24] of such systems. [For the WKB analysis of the energies corresponding to or-

bits that bounce off the "hard" inner wall, one must use (n_r+1) in place of $(n_r+3/4)$ in Eq. (16).] While $m=0$ states are allowed, the special central, zero-momentum initial state is not, and whether a pattern of something like the $T_{rev}^{(m\neq0)}$ revivals is supported is currently under study.

APPENDIX A

We briefly consider the special case of a Gaussian wave packet [of the form in Eq. (33)] with vanishing momentum, and initially located at the center of a two-dimensional square infinite well (or billiard) of dimension $L\times L$. Because the problem is entirely separable, the autocorrelation function for the 2D problem will be a product of the individual 1D values, namely, $A(t)=A_x(t)A_y(t)$, so it suffices to consider the 1D case. The energy eigenstates and eigenvalues are given as

$$u_n(x)=\frac{2}{L}\sin\left(\frac{n\pi x}{L}\right) \quad \text{and} \quad E_n=\frac{\hbar^2\pi^2n^2}{2mL^2} \quad \text{with}$$

$$n=1,2,3,4,\ldots$$

(A1)

[over the range $(0,L)$] and the general revival time is given by $T_{rev}=4mL^2/\hbar\pi$. For an initial Gaussian with vanishing momentum ($p_{0x}=0$) and located at the center of the well ($x_0=L/2$), the 1D expansion coefficients a_n simplify since the "odd" parity states (here meaning $n=2,4,\ldots$) make no contributions to the wave packet and the energies can be written in the form

$$E_n=\frac{\hbar\pi^2}{2mL^2}(2n-1)^2 \quad \text{with} \quad n=1,2,3,\ldots$$

(A2)

or as

$$E_n=\frac{\hbar^2\pi^2}{2mL^2}[4n^2-4n+1]=\frac{\hbar^2\pi^2}{2mL^2}[8n(n-1)/2+1]$$

$$=\left(\frac{2\pi\hbar}{T_{rev}}\right)8[\tilde{N}(n)+1/8],$$

(A3)

where $\tilde{N}(n)\equiv n(n-1)/2$ is an integer (neither even nor odd, in general). Just as with the $m=0$ case of the circular well, in this very special alignment, the modulus of $A(t)$ is unity with a reduced revival time of $T_{rev}^{(center)}=T_{rev}/8$, with a predictable phase factor (due to the constant 1/8 term) at integral multiples of $T_{rev}^{(center)}$. If one moves away from this special case by having $x_0\neq L/2$ or $p_0\neq0$, this special revival structure is lost and only the (still exact) T_{rev} revivals are evident.

We illustrate this in Fig. 4 for the case of a central, no-momentum solution (a) and for $x_0\neq L/2$ (b) and $p_0\gtrsim0$ (c) cases. We also show in the bottom (d) of Fig. 4, another
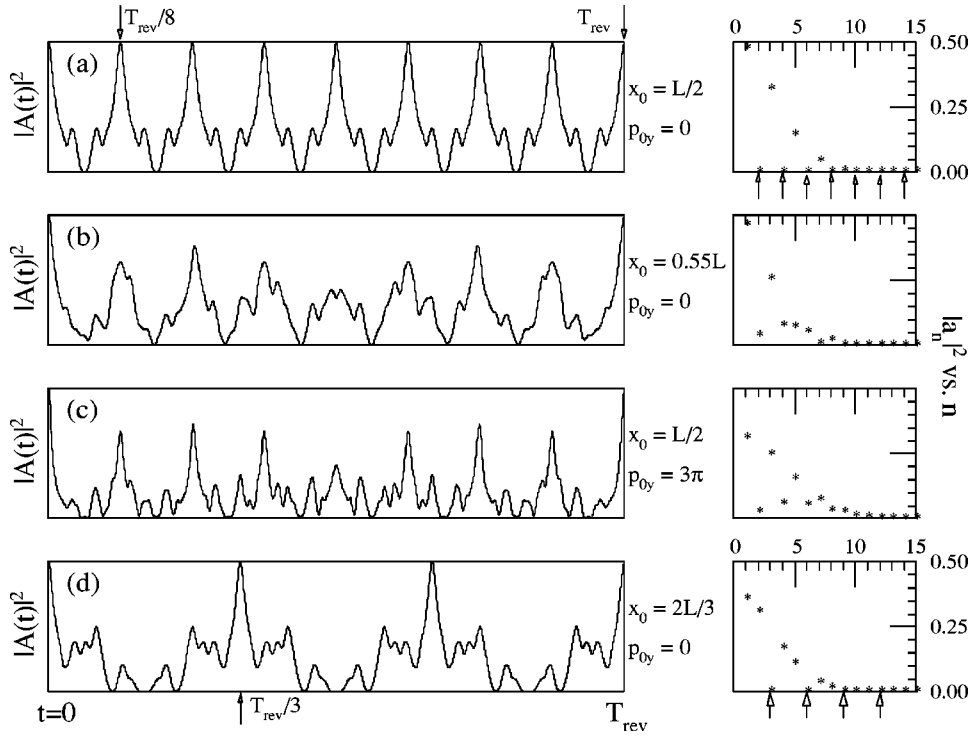
FIG. 4. Plots of the one-dimensional autocorrelation function $A(t)$ vs t, for various Gaussian wave packets in a one-dimensional infinite well defined over the length $(0,L)$. For case (a), where $x_0=L/2$ and $p_0=0$, there are special revivals at $T_{rev}/8$ due to the extra symmetries forcing all even expansion coefficients to vanish. The values of $|a_n|$ are shown directly to the right, with arrows indicating those that vanish identically for symmetry reasons. Cases (b) and (c), respectively, show the effect of changing x_0 and p_0 slightly away from the values in case (a), illustrating how only the "true" revival time is maintained. In case (d), we show another special case ($x_0=L/3$), where certain a_n vanish (every third one in this case) for symmetry reasons, also giving accidental revival times.

special case where certain expansion coefficients vanish for symmetry reasons in the no-momentum case ($x_0=2L/3$, where every third a_n is zero) with exact revivals at integral multiples of $T_{rev}/3$. Thus, a no-momentum 2D Gaussian wave packet moved slightly away from, say, $(x_0,y_0)=(2L/3,L/3)$ would experience the same kind of "broken" revival time symmetry, as one moved from the center.

A similar set of "accidental" or "symmetry" revival times exists for the equilateral triangle billiard. For example, for a zero-momentum state placed at the geometrical center, the revival time is $T_{rev}/9$, where T_{rev} is the exact revival time in Eq. (7). Similar "symmetry" points exist at distances of $\sqrt{3}L/12$ from the center in the direction of each vertex where the revival times are $T_{rev}/4$. Not surprisingly, we find no such additional "symmetry" points (besides the center) in the circular case.

APPENDIX B

While we have focused on the longer-term, revival dependence of wave packets in the circular well, it is interesting to note how the information about the classical closed (or periodic) orbits in this system is encoded in the energy eigenvalue spectrum, especially since most of the experimentally observed 2D circular billiard systems [18,19] have made measurements that are relevant for short-term, quasiclassical ballistic propagation. Such closed orbits are also the ones of relevance to periodic orbit theory [17] measurements of such billiard systems.

For a system with two quantum numbers, there are two classical periods [11], which in our case are given by

$$T_{cl}^{(n_r)} \equiv \frac{2\pi\hbar}{\partial E/\partial n_r} \quad \text{and} \quad T_{cl}^{(m)} \equiv \frac{2\pi\hbar}{\partial E/\partial m}, \qquad (B1)$$

and the two periods can beat against each other to produce the classical periodicity (T_{cl}^{po}) for closed or periodic orbits if they satisfy

$$pT_{cl}^{(n_r)} = T_{cl}^{(po)} = qT_{cl}^{(m)} \qquad (B2)$$

with $p>2q$ for this geometry. We can then use this formalism to understand how these conditions can give rise to the classical expressions for the minimum radius and path lengths in Eq. (50). Instead of using the approximate expression in Eq. (45) for the (m,n_r)-dependent energies, we make use of the WKB condition in Eq. (16) and simply take partial derivatives of both sides with respect to n_r and m, respectively. We thus obtain the conditions

$$\sqrt{\frac{\mu}{2\hbar^2}}\left[\int_{R_{min}}^{R} \frac{dr}{\sqrt{E - m^2\hbar^2/2\mu r^2}}\right]\left(\frac{\partial E}{\partial n_r}\right) = \pi, \qquad (B3)$$

$$\sqrt{\frac{\mu}{2\hbar^2}}\left[\int_{R_{min}}^{R}\frac{dr}{\sqrt{E-m^2\hbar^2/2\mu r^2}}\left(\frac{\partial E}{\partial n_r}-\frac{|m|\hbar^2}{\mu r^2}\right)\right]=0.$$
$$(B4)$$

The condition to be satisfied for periodic orbits can then be written as

$$\frac{q}{p}=\frac{T_{cl}^{(n_r)}}{T_{cl}^{(m)}}=\frac{(\partial E/\partial m)}{(\partial E/\partial n_r)}=\left(\frac{|m|\hbar}{\pi\sqrt{2\mu E}}\right)\left[\int_{R_{min}}^{R}\frac{dr}{r\sqrt{r^2-R_{min}^2}}\right].$$
$$(B5)$$

Evaluating the integral and using $R_{min}\equiv|m|\hbar/\sqrt{2\mu E}$, we find that

$$\frac{q}{p}=\frac{1}{\pi}\sec^{-1}\left(\frac{R}{R_{min}}\right)\quad\text{or}\quad R_{min}(p,q)\equiv R_{min}=R\cos\left(\frac{\pi q}{p}\right)$$
$$(B6)$$

is the condition on periodic orbits, as expected. To find the classical period for such closed orbits, we note that

$$T_{cl}^{(po)}=pT_{cl}^{(n_r)}=\frac{2\pi\hbar p}{(\partial E/\partial n_r)}$$

$$=(2p\sqrt{R^2-R_{min}^2})\sqrt{\frac{\mu}{2E}}=\frac{[2pR\sin(\pi q/p)]}{v_0}$$

$$=\frac{L(p,q)}{v_0},$$
$$(B7)$$

where we identify $v_0=\sqrt{2E/\mu}$ with the classical speed.

The classical periods for the closed orbits for the 2D annular well mentioned above can also be obtained from the WKB approximation in the same way, including those for the features corresponding to ''bounces'' off the inner infinite wall when R_{min} is replaced by R_{inner} in the integrations. The classical periods for the closed orbits for the 2D square and equilateral triangle billiards can, of course, also be obtained in an identical manner, using the exact results for their energies.

[1] M. Gutzwiller, *The Interplay Between Classical and Quantum Mechanics* (American Association of Physics Teachers, College Park, MD, 2001).

[2] M. Brack and R. K. Bhaduri, *Semiclassical Physics* (Addison-Wesley, Reading, MA, 1997).

[3] G. Alber and P. Zoller, Phys. Rep. **199**, 231 (1991).

[4] For Rydberg atoms, Z.D. Gaeta, M.W. Noel, and C.R. Stroud Jr., Phys. Rev. Lett. **73**, 636 (1994); for Stark wave packets, R. Bluhm, V.A. Kosteleckỳ, and B. Tudose, Phys. Rev. A **55**, 819 (1997); for alkali-metal atoms, R. Bluhm and V.A. Kosteleckỳ, *ibid.* **51**, 4767 (1995); for the Jaynes-Cummings model, I.Sh. Averbukh, *ibid.* **46**, R2205 (1992); for wave packets in a Morse-type potential well, S.I. Vetchinskin and V.V. Eryomin, Chem. Phys. Lett. **222**, 394 (1994); for an atom in a gravity well, W. -Y. Chen and G.J. Milburn, Phys. Rev. A **51**, 2328 (2995); J. Gea-Banacloche, Am. J. Phys. **67**, 776 (1999).

[5] D.L. Aronstein and C.R. Stroud, Jr., Phys. Rev. A **55**, 4526 (1997).

[6] P. Stifter, W. E. Lamb, Jr., and W. P. Schleich, in *Proceedings of the International Conference on Quantum Optics and Laser Physics*, edited by S. Y. Zhu, M. S. Zubairy, and M. O. Scully (Springer, Singapore, 1997), pp. 236–246.

[7] R. Bluhm, V.A. Kosteleckỳ, and J. Porter, Am. J. Phys. **64**, 944 (1996).

[8] F. Grossmann, J.-M. Rost, and W.P. Schleich, J. Phys. A **30**, L277 (1997).

[9] R.W. Robinett, Am. J. Phys. **68**, 410 (2000).

[10] D.F. Styer, Am. J. Phys. **69**, 56 (2001).

[11] R. Bluhm, V. Alan Kostelecký, and B. Tudose, Phys. Lett. A **222**, 220 (1996).

[12] G.S. Agarwal and J. Banerji, Phys. Rev. A **57**, 3880 (1998).

[13] P.J. Richens and M.V. Berry, Physica D **2**, 495 (1981); M.V. Berry and M. Wilkinson, Proc. R. Soc. London, Ser. A **392**, 15 (1984).

[14] A version of this problem is also discussed in J. Mathews and R. L. Walker, *Mathematical Methods of Physics*, 2nd ed. (Benjamin, Menlo Park, 1970), pp. 237–239.

[15] M.C. Gutzwiller, J. Math. Phys. **11**, 1791 (1970).

[16] R. Balian and C. Bloch, Ann. Phys. **69**, 76 (1972).

[17] H.-J. Stöckmann and J. Stein, Phys. Rev. Lett. **64**, 2215 (1990); E. Doron, U. Smilansky, and A. Frenkel, *ibid.* **65**, 3072 (1990); S. Sridhar and E.J. Heller, Phys. Rev. A **46**, R1728 (1992).

[18] C.M. Marcus, A.J. Rimberg, R.M. Westervelt, P.F. Hopkins, and A.C. Gossard, Phys. Rev. Lett. **69**, 506 (1992).

[19] N. Friedman, A. Kaplan, D. Carasso, and N. Davidson, Phys. Rev. Lett. **86**, 1518 (2001).

[20] See, e.g., *Handbook of Mathematical Functions*, edited by M. Abramowitz and I. A. Stegun (McGraw-Hill, New York, 1964), p. 364.

[21] A. B. Migdal and V. Krainov, *Approximation Methods in Quantum Mechanics* (Benjamin, New York, 1992), pp. 106–115.

[22] R. Bluhm and V.A. Kostelecký, Phys. Rev. A **50**, R4445 (1994).

[23] M. Nauenberg, J. Phys. B **23**, L385 (1990).

[24] K. Richter, D. Ullmo, and R.A. Jalabert, Phys. Rep. **276**, 1 (1996); S.M. Reimann, M. Brack, A.G. Magner, and M.V.N. Murthy, Surf. Rev. Lett. **3**, 19 (1996); R.W. Robinett, *ibid.* **5**, 519 (1998); see also Ref. [2].